Raman Study of the Anomalous TO Phonon Structure in GaP with Controlled Isotopic Composition

F. Widulle, T. Ruf, A. Göbel, E. Schönherr, and M. Cardona

Max-Planck-Institut für Festkörperforschung, Heisenbergstrasse 1, D-70569 Stuttgart, Germany

The transverse optical (TO) phonon in GaP has been measured in crystals with varying Ga isotopic composition by means of Raman scattering. In high resolution experiments at low temperature, we find a striking double peak structure in the line shape of natural GaP which varies with the Ga isotope abundance in a systematic manner. We calculate the spectra assuming anharmonic interaction of the TO phonon with a band of acoustic modes given by a model two-phonon density of states. This approach explains the measured Raman profiles and the isotope effects. [S0031-9007(99)09441-7]

Raman investigations of (stable) isotope effects have been started with germanium and diamond and extended recently to a variety of elemental as well as binary compound semiconductors. In these systems, isotope substitution offers new possibilities to understand phonon properties in detail. For recent reviews, see [1,2], and references therein. In the work reported here, we resolve a previously not observed fine structure in the Raman spectrum of the transverse optical (TO) phonon of GaP and use isotope replacement as a simple and powerful means to investigate this anomalous line shape. It is found to originate from anharmonic coupling of the TO Raman phonon with a continuum of two-phonon states. Our measurements and calculations show that disorder due to defects or isotope mass fluctuations is not responsible for the unusually large broadening of the TO line shape in natural GaP (^{nat}GaP) which was suggested earlier [2,3].

The phonon frequencies of an elemental and isotopically pure semiconductor with isotope mass M_i obey, in harmonic approximation, the mass dependence $\omega \propto M_i^{-1/2}$ at zero temperature which is valid for all phonon branches in the entire Brillouin zone. Many elements found in nature, however, consist of more than one stable isotope and possess a characteristic isotopic composition. In such systems, the *virtual crystal approximation* (VCA), which replaces the individual isotope mass, M_i, by the average mass, $\overline{M}$, is applied. *Anharmonic phonon-phonon interactions* also depend on the isotopic composition and affect the phonon properties. Isotope effects beyond those found within the VCA arise from the fact that the isotopes are usually distributed randomly in the crystal lattice and, thus, a certain degree of *isotope mass disorder* is present [1,2]. Both mechanisms—*anharmonicity* and *mass disorder*—lead to *additional line shifts* of the harmonic Raman frequency and *determine the broadening* of the observed spectral peaks. It is not known *a priori* which mechanism contributes predominantly.

In general, the above contributions to changes in the Raman spectrum also apply to binary compounds. Moreover, in these materials the average isotope mass *and* the individual isotope disorder of each sublattice can be tuned. In contrast to elemental semiconductors, the mass dependence of phonon frequencies in compounds varies continuously with the wave vector along a specific branch. This property has been exploited recently to determine phonon eigenvectors from the measured frequency shifts induced by isotope substitution [4]. In GaP only the Ga sublattice can be modified since phosphorus is an isotopically pure element (^{31}P).

The TO and longitudinal optic (LO) phonons in ^{nat}GaP have been studied earlier under variation of temperature [3] and pressure [5]. The TO phonon line exhibits a strong asymmetry (shoulder) to the low-energy side at room temperature, first observed by Barker [6]. The occurrence of this shoulder was attributed, at high temperatures, to anharmonic interaction of the TO(Γ) phonon with a nearly degenerate band of combined transverse and longitudinal acoustic (TA + LA) states around the X and K points of the Brillouin zone [5–7]. Weinstein tuned the spectral position of the low-energy shoulder at $T = 300$ K with respect to the main peak by applying hydrostatic pressure [5]. This led to a reduction of the asymmetry reflecting the loss of resonance between TO(Γ) and the two-phonon combinations TA + LA. In Ref. [3] the TO Raman line was considered to be nearly symmetric at low temperature, and only disorder due to defects in the crystal was assumed to be responsible for the broadening, while neglecting the influence of anharmonicity. Our new high-resolution experiments at $T = 6$ K show that a significant asymmetry of the TO Raman profile of ^{nat}GaP exists also at low temperature. Furthermore, the spectrum exhibits a striking double peak structure with a narrow splitting of approximately 1 cm^{-1}. A similar Raman line shape is clearly found in all investigated samples.

The samples were unoriented bulk crystals grown from Ga-P solution at 1340 K with typical dimensions of several hundred microns. Natural Ga (^{nat}Ga) contains 60.11% ^{69}Ga and 39.89% ^{71}Ga [8]. In addition to the ^{nat}GaP specimens, two isotopically pure crystals with highly enriched contents of ^{69}Ga (99.7%) and ^{71}Ga (99.6%) were grown.

Another isotopically disordered "antinatural" sample ($\overline{\text{nat}}$GaP) with an isotopic Ga composition of $^{69}\text{Ga}_{0.4}$-$^{71}\text{Ga}_{0.6}$, complementary to that of $^{\text{nat}}$Ga, allows us to better interpolate between the data of the isotopically pure crystals and probe possible disorder effects.

First-order Raman spectra were recorded in backscattering configuration using a microscope and a cold finger cryostat. The red 6764.4 Å krypton laser line was used for excitation, and low power densities were applied. Because of the transparency of GaP in the red part of the visible spectrum, heating effects are not expected and have not been observed. The scattered light was dispersed in a DILOR XY triple-grating spectrometer in the high-dispersion mode, yielding a spectral resolution of 0.25 cm^{-1}. For calibration purposes, the neon emission line at 6929.467 Å, corresponding to a frequency shift of 352.15 cm^{-1} with respect to the laser line, was measured simultaneously with the phonon spectra which were read out by a charge-coupled device detector.

Figure 1 shows the measured low temperature TO Raman spectra (symbols) together with the results of line shape calculations (solid lines) and the respective two-phonon density of states (DOS, dashed lines). The ver-
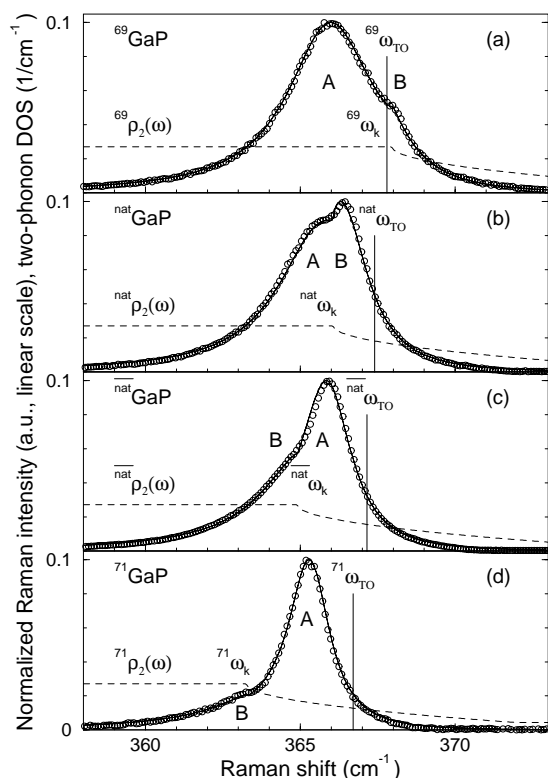

FIG. 1. Raman spectra of the TO phonon of (a) ^{69}GaP, (b) $^{\text{nat}}$GaP ($^{69}\text{Ga}_{0.6}{}^{71}\text{Ga}_{0.4}$P), (c) $\overline{\text{nat}}$GaP ($^{69}\text{Ga}_{0.4}{}^{71}\text{Ga}_{0.6}$P), and (d) ^{71}GaP at $T = 6$ K. The solid lines are fits to the experimental data (symbols) using the indicated two-phonon DOS, $\rho_2(\omega)$, (dashed lines), respectively. The vertical lines at ω_{TO} represent the δ-function peaks of the harmonic TO phonons prior to renormalization. See text for details.

tical lines represent the δ-function-like peaks that would correspond to the *bare* harmonic TO phonon at ω_{TO}. The Raman lines of all investigated samples are nonsymmetric *and* shoulders are observed even on a *linear* intensity scale unlike, e.g., in Refs. [5,6] where a *log* scale was used to visualize the asymmetry in the spectra recorded at $T = 300$ K. In the following, we denote these spectral features by A and B, as shown in Fig. 1, referring to the main peak and shoulder positions, respectively. Note that, for reasons which will become clear below, peak A in $^{\text{nat}}$GaP does not correspond to the intensity maximum. In fact, while the position of peak A tends to decrease only slightly with increasing Ga mass, feature B exhibits much stronger shifts. Compared to the LO phonon and most Raman phonons in other semiconductors [1,2], the TO phonon in GaP is unusually broad even at low temperature, and its width does not increase significantly up to room temperature [3,9]. Isotope disorder has been conjectured to explain this behavior, in analogy to recent observations for ZnSe [2,10]. However, the experiments presented here do not corroborate this suggestion, since the linewidths of the two isotopically pure samples with almost zero mass disorder are also quite large and, intriguingly, they differ significantly by almost a factor of 2 (see Fig. 1).

We therefore calculate the Raman spectrum of the TO phonon based on the assumption that solely third-order anharmonicity causes the broadening. This calculation is equivalent to a renormalization of the δ-function-like harmonic TO phonon by the interaction with the acoustic two-phonon DOS. This approach is supported by the previous investigations [5,6] and *ab initio* calculations [11] where TO(Γ) $\rightarrow$ LA + TA near X is proposed to be the main decay channel in GaP.

For a mathematical description of the renormalized quasiparticle, we use the complex phonon self-energy, $\Sigma(\omega) = \Delta(\omega) - i\Gamma(\omega)$, whose imaginary part [12] is directly proportional to the two-phonon DOS, $\rho_2(\omega)$,

$$\Gamma(\omega) = |V_3|^2 \rho_2(\omega). \qquad (1)$$

V_3 is the effective (i.e., including prefactors) third-order anharmonic coupling constant given in Ref. [12], which is assumed to be **q** independent. The real part, $\Delta(\omega)$, reflects the correction to the phonon frequency, whereas the imaginary part, $\Gamma(\omega)$, gives the broadening of the Raman line. A Kramers-Kronig transformation yields

$$\Delta(\omega) = \frac{2}{\pi} |V_3|^2 \int_0^\infty \frac{\omega' \rho_2(\omega')}{\omega^2 - \omega'^2} \, d\omega'. \qquad (2)$$

The renormalized Raman line shape [13] is given by

$$I(\omega) \propto \frac{\Gamma(\omega)}{[\omega - \omega_{\text{TO}} - \Delta(\omega)]^2 + [\Gamma(\omega)]^2}. \qquad (3)$$

Equation (3) is strongly influenced by the frequency dependence of the self-energy. In the following we show that the renormalization implicit in Eq. (3) distorts

the Lorentzian line shape and leads to the observed asymmetries.

To evaluate Eqs. (1)–(3), we use the histogramlike two-phonon DOS of Ref. [14] shown as a solid line in Fig. 2(a) which was derived from lattice-dynamical calculations. However, the steps of the histogram are too coarse (low energy resolution) for our purposes since discrete jumps in the DOS, in particular, near the phonon frequency under investigation, are reflected in the Raman line shape as additional spurious features. To avoid such artifacts, we smoothen the calculated DOS around ω_{TO} (dotted line in the inset in Fig. 2) retaining as the main feature a kink at ω_k that lies near ω_{TO}. We assume a constant value of the DOS for frequencies below the kink and a Van-Hove-type decrease ($\rho_2 \propto \sqrt{\omega - \omega_k}$) towards higher frequencies and normalize this model DOS according to $\int_0^\infty \rho_2(\omega) \times d\omega = 36$. For reasons explained below, we chose a slightly steeper decrease of $\rho_2(\omega)$ for $\omega > \omega_k$ than suggested by the calculated DOS. Figure 2(b) displays $\Delta(\omega)$ calculated from $\rho_2(\omega)$ with this analytical approximation around ω_{TO} and a typical value of $|V_3|^2 = 57$ cm^{-2} (see below). The large pileup of the DOS above 400 cm^{-1} implies $\Delta(\omega) < 0$ near the TO frequency. This renormalization reduces ω_{TO} by about -1.5 cm^{-1} and overcompensates a positive frequency shift which is expected from the asymmetric DOS near and below ω_{TO} [see Fig. 2(a)].

In an iterative procedure, we adjust the parameters ω_{TO}, ω_k, and $|V_3|^2$ and simulate the experimental spectra until we obtain optimum visual agreement with the data (see solid lines in Fig. 1). We find that the kinks (ω_k) in the

two-phonon DOS are close to the features B of the Raman line shapes. The frequencies ω_{TO} and ω_k obtained from the fits are plotted as open symbols in Fig. 3. With increasing Ga mass, they show a steady decrease with significantly different slopes (dashed lines to guide the eye). This observation can be explained as follows: in the harmonic approximation, the zone-center optical mode frequency depends on the reduced mass $\mu_{GaP}^{-1} = \overline{M}_{Ga}^{-1} + M_P^{-1}$ and scales like $\omega(\Gamma) \propto \mu_{GaP}^{-1/2}$, whereas acoustic mode frequencies at the X point are proportional to $\overline{M}_{Ga}^{-1/2}$ (in a first approximation). We illustrate this scaling behavior by means of the thin solid lines in Fig. 3 with the values for ^{71}GaP as reference points, since in this sample almost no disorder is present, and the line shape renormalization should be little. These predictions are in good agreement with the dashed lines connecting the respective values of ω_{TO} and ω_k. The deviations from the ideal harmonic behavior can be mainly attributed to deficiencies in the analytical approximation of $\rho_2(\omega)$ near ω_{TO}. Further modifications are expected from the fact that TA modes are involved, where $\omega_k \propto \overline{M}_{Ga}^{-1/2}$ does not hold strictly. The TO(Γ) mode might also interact with numerous states along the X-K line which have a different mass-frequency relation. Note that these significantly different mass dependences of ω_{TO} and ω_k make it possible to perform the present study; otherwise no changes in the Raman line shape would be observed. From the fact that ω_{TO} and ω_k of the disordered crystals ^{nat}GaP and $\overline{^{nat}}$GaP interpolate
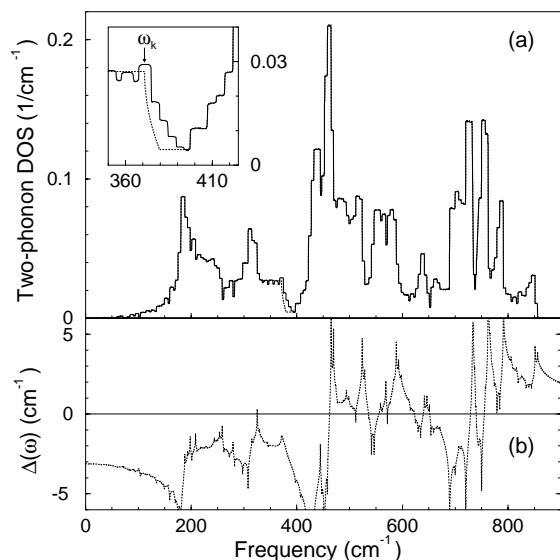

FIG. 2. (a) Calculated two-phonon DOS, $\rho_2(\omega)$, for GaP (solid line) from Ref. [14] used to simulate the Raman spectra. Near $\omega_{TO} \approx 366$ cm^{-1} this $\rho_2(\omega)$ was replaced by an analytical approximation (dotted line; see inset) to avoid artifacts. (b) Real part of the phonon self-energy, $\Delta(\omega)$, as calculated from the modified two-phonon DOS using $|V_3|^2 = 57$ cm^{-2}.
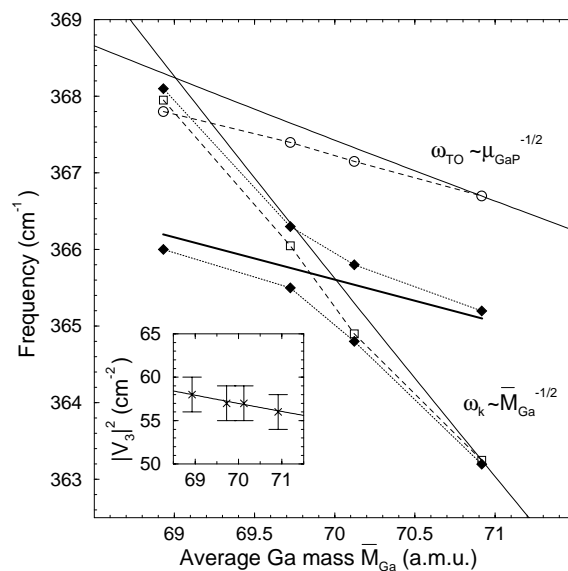

FIG. 3. Mass dependences of the bare TO frequency, ω_{TO}, the kink frequency in the two-phonon DOS, ω_k, and the anharmonic coupling constant $|V_3|^2$ (inset). The symbols ($\bigcirc, \square, \times$) are results from fits of ω_{TO}, ω_k, and $|V_3|^2$ to the experimental data. The thin solid lines are theoretical mass dependences for the respective parameters. The filled diamonds display the measured frequencies of the spectral features A and B of the TO Raman spectrum. See text for details.

the values of the isotopically pure samples almost linearly, we conclude that effects of mass *disorder* on the phonon renormalization are negligible.

The filled diamonds in Fig. 3, connected by the thin dotted lines to guide the eye, represent the characteristic frequencies determined from the measured (renormalized) TO line shapes, i.e., of both peak A and feature B. The intensity maxima of ^{69}GaP and ^{71}GaP (peak A) closely correspond to renormalized TO phonons which experience only little disturbance by the kink in $\rho_2(\omega)$. Their positions with respect to the bare ω_{TO} are mainly determined by the constant negative shift of about -1.5 cm^{-1} mentioned above [see Fig. 2(b)]. Between these Ga masses the TO phonon crosses the kink that causes the observed strong peak distortions. Accordingly, a situation similar to a level anticrossing occurs for the mass dependences of peak A and feature B in the Raman line shapes: peak A for $\overline{M}_{Ga} = 69$ changes from opticlike to acousticlike behavior with increasing Ga mass and turns into feature B for $\overline{M}_{Ga} = 71$. Feature B behaves vice versa [acousticlike for $\overline{M}_{Ga} = 69$ and opticlike (A) for $\overline{M}_{Ga} = 71$]. The renormalized TO frequency would follow the thick solid line in Fig. 3 in the case of a mere crossing without interaction. This result demonstrates that the description of the Raman line shape in terms of a frequency shift and a linewidth becomes ill-defined for ^{nat}GaP: the spectral dependence of $\Delta(\omega)$ and $\Gamma(\omega)$ has to be taken into account. Because of the strong distortion of the spectrum a single value for the TO frequency cannot be assigned. In other more extreme cases, anharmonic renormalization of the TO phonon results in richly structured and very broad TO Raman spectra, e.g., in CuCl, where a Fermi resonance occurs [13].

The values for $|V_3|^2$ found from the fits are shown in the inset of Fig. 3 (symbols). The general mass dependence of V_3 is given in Ref. [12] and can be estimated in our case by the product of the approximate individual mass dependences of the three phonons participating in the anharmonic scattering process, namely, TO(Γ), LA(X), and TA(X):

$$|V_3|^2 \propto \mu_{GaP}^{-1/2}\overline{M}_{Ga}^{-1/2}\overline{M}_{Ga}^{-1/2}. \qquad (4)$$

This behavior is shown by the solid line in the inset in Fig. 3. The values of $|V_3|^2$ around 57 cm^{-2} indicate a reduced anharmonic coupling strength compared to $|V_3|^2 = 70$ cm^{-2} obtained for the more ionic CuCl [13].

Note that fits of lattice-dynamical models to inelastic neutron scattering data must be very accurate near TO(Γ) and the LA and TA frequencies along X-K in order to provide a realistic two-phonon DOS around TO(Γ). Conversely, our Raman experiments can be used as an extremely sensitive tool for probing details of the two-phonon DOS and to either verify or falsify different lattice-dynamical models. To test the quality of the analytical approximation of the DOS near ω_k, we have performed model calculations for kinks with varying steepness. The

shallower decline of $\rho_2(\omega)$ for $\omega > \omega_k$ suggested by [14] [solid line, Fig. 2(a)] leads to line shapes which do not fit the Raman data as well as those in Fig. 1. Furthermore, the fitted values of $|V_3|^2$ deviate significantly from the theoretically expected mass dependence, even when uncertainties in the three factors of Eq. (4), as outlined above, are considered.

In conclusion, we have found a new double peak structure in the Raman line shape of ^{nat}GaP which changes with altering the Ga isotopic composition and reflects both the real and the imaginary part of a frequency-dependent phonon self-energy. Isotope substitution is the method of choice for a systematic investigation since it allows a fine-tuning of the effect in highly resolved steps. The theoretical approach presented here, based on third-order anharmonic phonon-phonon interaction and a model two-phonon DOS, explains all measured low temperature Raman line shapes in remarkable detail. The individual mass dependences of the parameters ω_{TO}, ω_k, and $|V_3|^2$, which were not subject to restrictions during the fits, are consistent with known isotope effects. The results show that third-order anharmonicity is the dominant scattering mechanism in GaP at low temperature. Isotope disorder effects and higher-order anharmonic contributions seem to be unimportant. The results derived from this study are crucial for the interpretation of temperature dependent measurements, which are expected to reveal information about higher-order anharmonic terms. Such experiments have already been performed and will be presented elsewhere.

[1] M. Cardona, Physica (Amsterdam) **263B–264B**, 376 (1999).

[2] A. Göbel *et al.,* in Proceedings of the 24th International Conference on the Physics of Semiconductors (World Scientific, Singapore, to be published).

[3] B. Kh. Bairamov *et al.,* Sov. Phys. Solid State **16**, 1323 (1975).

[4] F. Widulle *et al.,* Phys. Rev. Lett. **82**, 3089 (1999).

[5] B. A. Weinstein, Solid State Commun. **20**, 999 (1976).

[6] A. S. Barker, Jr., Phys. Rev. **165**, 917 (1968).

[7] B. A. Weinstein and G. J. Piermarini, Phys. Rev. B **12**, 1172 (1975).

[8] J. Emsley, in *The Elements* (Clarendon Press, Oxford, 1991), 2nd ed., p. 77 or http://www.shef.ac.uk/chemistry/web-elements/

[9] W. E. Bron *et al.,* Phys. Rev. B **34**, 6961 (1986).

[10] A. Göbel *et al.,* Phys. Rev. B **59**, 2749 (1999).

[11] A. Debernardi, Phys. Rev. B **57**, 12 847 (1998).

[12] M. Balkanski *et al.,* Phys. Rev. B **28**, 1928 (1983).

[13] A. Göbel *et al.,* Phys. Rev. B **56**, 210 (1997).

[14] K. Kunc, Ann. Phys. (Paris) **8**, 319 (1973–1974).